Rotational properties of nondipolar and dipolar Bose-Einstein condensates confined in annular potentials

E. Ö. Karabulut,[1,2] F. Malet,[3] G. M. Kavoulakis,[4] and S. M. Reimann[1]
[1]*Mathematical Physics, LTH, Lund University, Box 118, SE-22100 Lund, Sweden*
[2]*Department of Physics, Faculty of Science, Selcuk University, TR-42075 Konya, Turkey*
[3]*Department of Theoretical Chemistry and Amsterdam Center for Multiscale Modeling, FEW, Vrije Universiteit, De Boelelaan 1083, 1081HV Amsterdam, The Netherlands*
[4]*Technological Educational Institute of Crete, Post Office Box 1939, GR-71004, Heraklion, Greece*
(Received 27 July 2012; revised manuscript received 8 December 2012; published 15 March 2013)

We investigate the rotational response of both nondipolar and dipolar Bose-Einstein condensates confined in an annular potential via minimization of the energy in the rotating frame. For the nondipolar case we identify certain phases which are associated with different vortex configurations. For the dipolar case, assuming that the dipoles are aligned along some arbitrary and tunable direction, we study the same problem as a function of the orientation angle of the dipole moment of the atoms.

DOI: 10.1103/PhysRevA.87.033615 PACS number(s): 03.75.Lm, 05.30.Jp

I. INTRODUCTION

In recent experiments on ultracold atomic gases, the confinement of atoms in toroidal traps has become possible [1]. In such confining potentials persistent currents have also been created and observed [2–5], in close analogy to semiconductor nanostructures [6,7]. The simplicity of these systems makes them ideal for studying effects associated with superfluidity, including, for example, rotational properties and persistent flow.

In another series of recent experiments it has become possible to trap atoms [8] and molecules [9] with a nonzero dipole moment. An important difference with respect to most of the previously realized experiments—in which the particles had zero dipole moment and the effective atom-atom interactions could be modeled with the usual contact term—is that in the dipolar case the interaction potential is long ranged and anisotropic. As a consequence, dipolar gases present new properties that allow for the study of interesting effects. In three dimensions, the head-to-tail alignment of the dipoles causes instabilities towards collapse [10], while low-dimensional confinement tends to make the system more stable [11]. Quasi-two- or quasi-one-dimensional confinement thus suppresses the instabilities associated with the dipolar interaction and is advantageous in that respect.

Recently, several properties of dipolar gases have been examined in effectively two-dimensional systems. Among these, the rotational properties of dipolar degenerate gases have received considerable attention. In particular, the rotational properties of dipolar Bose-Einstein condensates have been investigated in different confining geometries, including axially symmetric harmonic [12], elliptic harmonic [13], and toroidal traps [14–18]. Also, recently it has become possible to create a Bose-Einstein condensate of ^{164}Dy, with a magnetic moment roughly three times larger than ^{52}Cr, which increases the dipole coupling constant by approximately a factor of 10 [19].

Dipolar Bose-Einstein condensates confined in toroidal traps have been investigated both within the mean-field approximation [14] and in the few-particle limit [20]. These systems have been shown to exhibit some very interesting effects due to the interplay between the nontrivial topology of the ringlike confinement and the anisotropic nature of the dipole-dipole interaction. More specifically, when the dipole moment has a nonzero in-plane component, the effects associated with breaking the axial symmetry of the system have been shown to have potential applications in, e.g., Josephson-type oscillations and self-trapping phenomena [16,17,21].

Motivated by the experimental progress mentioned above on toroidal traps and on dipolar gases, we study the states of lowest energy in the rotating frame of a Bose-Einstein condensate that is confined in an annular potential, first considering a condensate that consists of nondipolar atoms [22–25] and then addressing the dipolar case. Our calculations are closely related with those of Ref. [26], which analyzed the lowest-energy state of a uniform (nondipolar) rotating superfluid confined in a hard-wall annulus. In this study it was shown that as the rotational frequency increases, initially there are vortices that are located in the region of zero density. Eventually the vortices start to form in the region of nonzero density, and finally the real vortices form a circular array, or even multiple arrays of vortices. These theoretical predictions were in good agreement with the experimental results on liquid helium that followed afterward [27]. In what follows below, we refer to the vortices that are located in the region of negligible density as “phantom” vortices and the ones that are located in the region of non-negligible density as “real” vortices.

The paper is organized as follows. In Sec. II we present our model. In Sec. III we investigate the rotational response of a nondipolar gas. In Sec. IV we investigate the effect of the dipolar interaction, assuming that the dipole moment of the atoms is oriented along some arbitrary direction due to an external polarizing field, which rotates with the trap. We demonstrate that the vortex configuration depends strongly on the orientation angle of the dipole moment of the atoms. Finally in Sec. V we summarize our results.

II. MODEL

The annular potential that we consider is modeled via a combination of harmonic potentials in the transverse direction

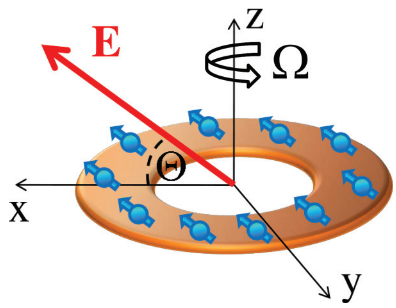

FIG. 1. (Color online) Schematic illustration of the rotating quasi-two-dimensional annular trap. The atoms move on the xy plane with an angular frequency Ω, which is along the z axis, in an annulus of mean radius R and a width that is set by the oscillator length $a_0 = \sqrt{\hbar/(M\omega_0)}$. In the case of dipolar atoms, their dipole moment is oriented on the xz plane, forming an angle Θ with the x axis due to an external (magnetic or electric) field $\mathbf{E}$, which is assumed to rotate with the same angular frequency as the trapping potential.

and in the direction perpendicular to the plane of motion of the atoms,

$$V(\mathbf{r}) = V_r(\mathbf{r}_\perp) + V_z(z) = \tfrac{1}{2}M\omega_0^2(r_\perp - R)^2 + \tfrac{1}{2}M\omega_z^2 z^2. \tag{1}$$

Here z is the symmetry axis of the trap, which is also the axis of rotation of the annulus. In addition $\mathbf{r}_\perp$ is the position vector on the xy plane, while ω_0 and ω_z are the trap frequencies. The ratio ω_z/ω_0 is chosen to be equal to 100, which makes the motion of atoms quasi-two-dimensional, since $\hbar\omega_z$ is the largest energy scale in the problem. The ratio R/a_0 is chosen equal to 4, where $a_0 = \sqrt{\hbar/(M\omega_0)}$ is the oscillator length that corresponds to the frequency ω_0 and mass M. Figure 1 shows schematically the corresponding annularlike potential and also the external field that is assumed to polarize the (dipolar) atoms. Without loss of generality, this field is taken to be on the xz plane, forming an angle Θ with the x axis, and assumed to rotate with the same angular frequency as the trapping potential.

Concerning the interactions, these are modeled via a short-range contact potential (for the short-range correlations) and the usual dipole-dipole potential, which describes the long-range part of the interaction. Because of the assumed strong confinement along the z axis, one may safely assume that the order parameter has the product form

$$\Psi(\mathbf{r}) = \Phi(\mathbf{r}_\perp)\phi(z), \tag{2}$$

where $\phi(z)$ is the Gaussian ground state of the harmonic potential $V_z(z)$. This assumption allows us to reduce the problem from three dimensions to two dimensions for the order parameter $\Phi(\mathbf{r}_\perp)$, which satisfies the Gross-Pitaevskii-like equation

$$\left[-\frac{\hbar^2\nabla_\perp^2}{2M} + V_r(\mathbf{r}_\perp) + V_{\rm dip}(\mathbf{r}_\perp) + g|\Phi(\mathbf{r}_\perp)|^2 - \Omega L_z\right]\Phi(\mathbf{r}_\perp) = \mu\Phi(\mathbf{r}_\perp). \tag{3}$$

In the above equation $g = (\hbar^2/M)\sqrt{8\pi}Na/a_z$, where N is the atom number, a is the scattering length for zero-energy elastic atom-atom collisions, and $a_z = \sqrt{\hbar/M\omega_z}$ is the oscillator length in the z direction. Also Ω is the rotational frequency of the trap, L_z is the operator of the angular momentum along the z axis, μ is the chemical potential, and

$$V_{\rm dip}(\mathbf{r}_\perp) = \int V_{\rm eff}(\mathbf{r}_\perp - \mathbf{r}'_\perp)\,|\Phi(\mathbf{r}'_\perp)|^2\,d\mathbf{r}'_\perp \tag{4}$$

is the effective dipolar interaction potential. Here $V_{\rm eff}(\mathbf{r}_\perp)$ is given by [in cylindrical polar coordinates, with $\mathbf{r}_\perp = (r_\perp,\phi)$] [28],

$$\begin{aligned} V_{\rm eff}(\mathbf{r}_\perp) = \frac{D^2}{\sqrt{8\pi}}\frac{e^{w/2}}{a_z^3}\Big\{&(2+2w)K_0(w/2) - 2wK_1(w/2) \\ &+ \cos^2\Theta\Big[-(3+2w)K_0(w/2) \\ &+ (1+2w)K_1(w/2)\Big] + 2\cos^2\Theta\cos^2\phi \\ &\times\Big[-wK_0(w/2) + (w-1)K_1(w/2)\Big]\Big\}. \end{aligned} \tag{5}$$

In the above equation $w \equiv r_\perp^2/2a_z^2$, and $K_0(w)$ and $K_1(w)$ are the zero-order and first-order modified Bessel functions of the second kind.

The problem thus reduces to solving the nonlocal and nonlinear integrodifferential Eq. (3). We solve it with use of a fourth-order split-step Fourier method within an imaginary-time propagation approach [29]. Within this method one starts with some initial state, which then propagates in imaginary time until numerical convergence is achieved.

III. NONDIPOLAR ATOMS IN A ROTATING ANNULAR TRAP

We first consider the case of nondipolar atoms and vary the rotational frequency Ω for a fixed interaction strength, choosing $Mg/\hbar^2 = \sqrt{8\pi}Na/a_z = 150$. Since the ratio between the interaction energy and $\hbar\omega_0$ is approximately $Naa_0/(a_zR) \sim 10$, and also $\omega_z/\omega_0 = 100$, there is a clear hierarchy of energy scales, with $\hbar\omega_z$ being roughly 10 times as large as the interaction energy, which in turn is roughly 10 times as large as $\hbar\omega_0$. Therefore, while the cloud is in the ground state of the harmonic oscillator along the z direction, it is closer to the Thomas-Fermi limit in the direction along the plane of motion.

Using the numerical procedure outlined above, the energetically favorable state of the cloud is determined in the rotating frame for a certain value of Ω. In our simulations we have considered initial conditions with different values of the winding number in order to make sure that the states that we have found are indeed the ones of lowest energy in the rotating frame. As the rotational frequency of the trap Ω increases, we observe that initially there is a critical value Ω_c where a "phantom" vortex state forms, which is located at the trap center, as seen in Fig. 2(a). This phantom vortex is a state of quantized circulation, which does not break the axial symmetry of the density distribution of the cloud. The phase of the order parameter acquires a jump of 2π, while phantom vortices tend to make the gas expand in the radial direction due to the centrifugal force [22]. For the parameters that we have used, $\Omega_c/\omega_0 \approx 0.036$. If one approximates the annulus to a one-dimensional ring of radius R, then $\Omega_c = \hbar/(2MR^2)$, which implies that $\Omega_c/\omega_0 = 1/32 = 0.03125$, in rather good agreement with our numerical result.

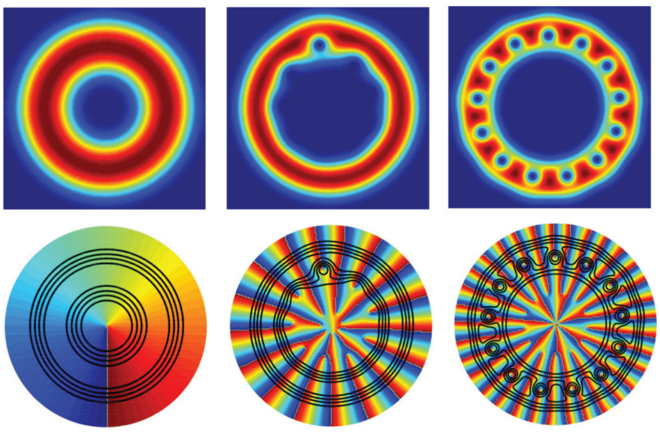

FIG. 2. (Color online) Density and phase of the order parameter corresponding to three frequencies for the nondipolar case ($D = 0$) and $\sqrt{8\pi}Na/a_z = 150$. For (a) $\Omega/\omega_0 = \Omega_c/\omega_0 \approx 0.036$ a "phantom" vortex appears, for (b) $\Omega/\omega_0 \approx 0.53$ there is a "real" vortex, and for (c) $\Omega/\omega_0 \approx 0.63$ there is an array of vortices along the annulus.

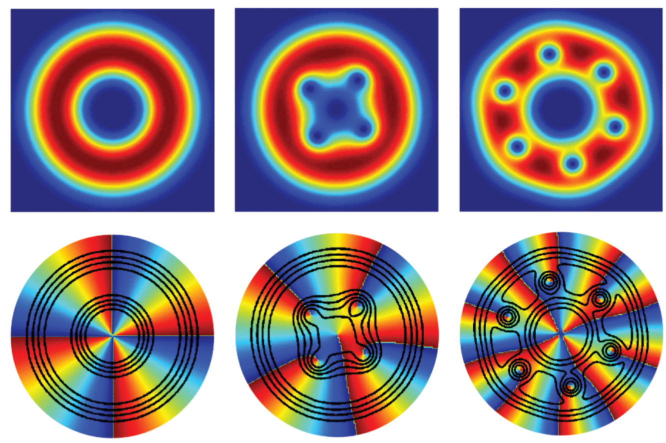

FIG. 3. (Color online) Density and phase of the order parameter corresponding to three frequencies for the nondipolar case ($D = 0$) and $\sqrt{8\pi}Na/a_z = 150$. For (a) $\Omega/\omega_0' = 0.18$ there are four "phantom" vortices, for (b) $\Omega/\omega_0' = 0.19$ there is one phantom and four "real" vortices, and for (c) $\Omega/\omega_0' = 0.25$ there are four phantom vortices and an array of six vortices along the annulus. Here $\omega_0' = \omega_0/2$.

As Ω increases further, more phantom vortices accumulate inside the annulus. Eventually, one of these vortices penetrates the annulus, giving rise to a "real" vortex state, as shown in Fig. 2(b). According to our results, this state actually penetrates the cloud from the center of the annulus. The point (in the angular direction) where the vortex enters the cloud is arbitrary (in the sense that the configuration of real and phantom vortices in the plots of Fig. 2 can be rotated by an arbitrary angle), as the symmetry of the Hamiltonian is broken spontaneously. We have found that this vortex state starts to penetrate the annulus at $\Omega/\omega_0 \approx 0.53$.

Finally, there is a third phase, where an array of vortices forms along the annulus, as seen in Fig. 2(c). At $\Omega/\omega_0 \approx 0.63$, we have determined that this lattice is roughly located at the center of the annulus. The last two values of Ω that are given above are rather close to each other. To get an estimate of these frequencies we recall that for a sufficiently large number of vortices, the velocity field resembles that of solid-body rotation. It is well known that the line integral of the velocity field $\oint \mathbf{v} \cdot d\mathbf{l}$ around a closed loop that includes N_v vortex states is equal to $N_v\kappa$, where $\kappa = 2\pi\hbar/M$. For large values of N_v, solid-body rotation implies that $\mathbf{v} = \Omega r_\perp \hat{\phi}$ and therefore around a radius R, $2\pi\Omega R^2 = N_v\kappa$. The resulting mean-vortex density $N_v/(\pi R^2)$ is thus $2\Omega/\kappa$. The formation of real vortices is expected to take place when the mean vortex density becomes comparable to the width of the annulus d [26], which gives a frequency $\Omega \approx \kappa/\pi d^2$ (ignoring logarithmic factors), or $\Omega/\omega_0 \approx 2(a_0/d)^2$. From Fig. 2(c) d/a_0 is roughly $4/3$, and therefore $\Omega/\omega_0 \approx 1$.

Interestingly, the above-mentioned intermediate phase with a single vortex state that we have found in our calculations was not observed in the study of Ref. [22], which considered a similar problem. However, in that paper the authors modeled the annular potential with a harmonic minus quartic term, giving rise to a considerably wider annulus than the one produced by our shifted parabolic confinement. Indeed, in a harmonic potential it is well known that a single off-center vortex state cannot be stable in the rotating frame [30]. If one creates a narrow hole in the density of the cloud at the center of the trap, such a state is still unstable. This explains the absence of such a single vortex state for a wide annulus, as in Ref. [22]. Nevertheless, if the width of the annulus becomes narrow enough this state may become stable, as we have found in our imaginary-time propagation. We have also confirmed that this state is stationary by evolving it in real time. Furthermore, when the annulus is wide enough, i.e., for a smaller value of $\omega_0' = \omega_0/2$, with the rest of the parameters being the same as those of Fig. 2, we have found that there is no stable phase with a single real vortex state. Rather, with increasing Ω there is a direct transition from a state that has phantom vortices only, Fig. 3(a), to a state with one phantom and four real vortices, Fig. 3(b). For even higher rotational frequencies, Fig. 3(c), the system forms a regular vortex lattice, as in Fig. 2(c).

In a sufficiently narrow annulus a single off-center vortex state cannot be stable because of the form of the energy spectrum (for a repulsive effective interaction) [31]. Therefore our results imply the existence of a range of values for the width of the annulus that allow the stability of a single off-center vortex state.

IV. DIPOLAR CASE

We turn now to the case where the atoms have a nonzero dipole moment. In addition to the hard-core potential considered in the previous section, which is kept fixed with $Mg/\hbar^2 = \sqrt{8\pi}Na/a_z = 150$, we consider a dipolar interaction of a fixed strength. Introducing the dipolar length $a_{dd} \equiv MD^2/(3\hbar^2)$, we choose $a_{dd}/a = 2.505^2/3 \approx 2.092$. In the above expression $D^2 = d^2/(4\pi\epsilon_0)$ when the atoms have an electric dipole moment d, where ϵ_0 is the permittivity of the vacuum; when the atoms have a magnetic moment μ, $D^2 = \mu_0\mu^2/(4\pi)$, where μ_0 is the permeability of the vacuum. With this choice of parameters the dipolar and the contact interactions are of comparable magnitude.

We stress that while the results presented below are representative of a whole range of reasonable parameters, they do not in any way exhaust all the phases that one may find. The richness of the possible phases is due to the large number of free parameters, including the strength and sign of the contact potential, the strength of the dipolar interaction, the width of the annulus, the orientation angle of the polarizing field, the rotational frequency of the trap, and the atom number.

In this problem, small values of D and thus weak dipolar interactions may give rise to a very smooth energy surface, which leads to degeneracy problems in the calculation. On the other hand, large values of D tend to cure this problem; however, they also make the system unstable against collapse for small values of the angle Θ due to the head-to-tail alignment of the dipoles.

We investigate the rotational response of the cloud considering four values for the angle of the dipole moment, $\Theta = 0^\circ$, 30°, 60°, and 90°, as in Fig. 1. When $\Theta = 90^\circ$ the interaction respects the axial symmetry of the trapping potential and is also purely repulsive. As a result, the system behaves qualitatively as in the case of a contact potential alone, with a phantom vortex state, a real vortex state, and a vortex lattice forming with increasing Ω.

For any other value of the angle Θ, as Ω increases, initially the cloud still responds by forming one phantom vortex at the center of the trap, as in the nondipolar case. On the other hand, for higher rotational frequencies the gas behaves in a qualitatively different way. In this case the dipolar interaction breaks the axial symmetry of the Hamiltonian, introducing a preferred direction.

In Fig. 4 we plot the density and the phase of the order parameter for four values of the angle $\Theta = 0^\circ$, 30°, 60°, and 90°. The value of Ω in each case is the one for which the first real vortices form around the annulus. While for $\Theta = 90^\circ$ the position where the vortex enters the annulus is arbitrary (as in the nondipolar case), for all other values of Θ this is determined by the direction of the polarizing field, which is chosen to be in the direction going from the bottom to the top of the page. For $\Theta = 60^\circ$ and 30° there are actually two vortex states which enter the annulus from opposite ends. For $\Theta = 0^\circ$ instead of two vortices, there are two pairs of vortices, which are symmetrically displaced from the direction of the polarizing field. Actually, we have found that this behavior is not specific to $\Theta = 0^\circ$ only, but rather it persists up to roughly $\Theta = 10^\circ$.

In addition, as one can see from the phase of the order parameter, as Θ decreases the number of phantom vortices increases. The main reason for this is the fact that the rotational frequency increases, too. Especially for $\Theta = 0^\circ$ the number of vortices is very large because of the value of the rotational frequency, which is close to ω_0, $\Omega/\omega_0 \approx 0.80$. Also for the nondipolar case, $D = 0$, the number of vortices is comparable to the one seen in Fig. 4(a), with the only difference being that there is already an array of real vortices. Therefore, the main effect of the dipolar interaction is the suppression of real vortices. Also, with decreasing Θ the density at the center of the trap decreases. For $\Theta = 0^\circ$ the density in this region is extremely small and therefore it appears to be "empty" in Fig. 4, as can be seen also from the phase plot.

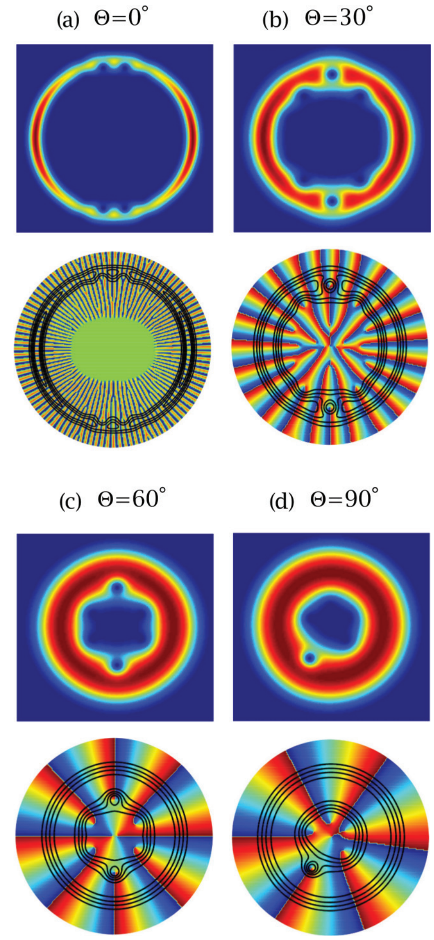

FIG. 4. (Color online) Density and phase of the order parameter corresponding to the dipolar case, with $\sqrt{8\pi} Na/a_z = 150$ and $a_{dd}/a_0 = 2.505^2/3$. For (a) $\Theta = 0^\circ$, $\Omega/\omega_0 \approx 0.80$, (b) $\Theta = 30^\circ$, $\Omega/\omega_0 \approx 0.5835$, (c) $\Theta = 60^\circ$, $\Omega/\omega_0 \approx 0.36$, and (d) $\Theta = 90^\circ$, $\Omega/\omega_0 \approx 0.296$. The polarizing field is chosen to be in the direction going from the bottom to the top of the page.

V. SUMMARY

In the present study we have investigated two problems. First, we studied the rotational response of a superfluid that is confined in an annular potential. Such a trapping geometry interpolates in a sense between one- and two-dimensional motion, depending on the ratio between the mean radius of the annulus and its width. The second problem we have addressed is the effect of the long-range and anisotropic character of the dipolar interaction.

Starting with the nondipolar case, as the rotational frequency of the annulus increases, there is a critical frequency above which a phantom vortex state appears in the region of essentially zero density, around the center of the trap. As the rotational frequency increases further, more phantom vortices start to reside in this region; however, these vortices do not affect the density in the axial direction. The number of the phantom vortices increases until it reaches a threshold.

Eventually, a vortex array or arrays form with increasing rotational frequency of the trap. In addition, provided that the width of the annulus is neither too large nor too small, it is found that an intermediate phase with a single off-center real vortex state may also be stable.

The dipolar case differs from the above mainly because of the symmetry breaking of the Hamiltonian due to the dipolar interaction (unless the dipole moment is perpendicular to the plane of motion of the atoms). Even the nonrotating system is affected by the dipole-dipole interaction, with the formation of one or two density maxima, depending on the value of the parameters, as seen in Refs. [12,14,15]. This inhomogeneity in the density affects also the critical rotational frequencies. Initially a phantom vortex still appears at the center of the trap. However, for larger rotational frequencies of the trap the real vortices penetrate the annulus either in pairs or in couples of pairs from opposite ends of the cloud in the direction of the polarizing field of the dipoles.

Rotating atomic Bose-Einstein condensates confined in toroidal potentials have been realized experimentally recently, while dipolar gases are under intense experimental investigation. As shown in the present article, the combination of these two effects—that should be accessible also experimentally—gives rise to interesting effects.

ACKNOWLEDGMENTS

We thank Alexander L. Fetter and Kimmo Kärkkäinen for very useful discussions. This work was financed by the Swedish Research Council and the Nanometer Structure Consortium at Lund University and originated from a collaboration within the POLATOM Research Networking Programme of the European Science Foundation (ESF). E.Ö.K. is supported by the Turkish Council of Higher Education (YÖK) within the scope of the Postdoctoral Research Scholarship Program.

[1] S. Gupta, K. W. Murch, K. L. Moore, T. P. Purdy, and D. M. Stamper-Kurn, Phys. Rev. Lett. **95**, 143201 (2005); S. E. Olson, M. L. Terraciano, M. Bashkansky, and F. K. Fatemi, Phys. Rev. A **76**, 061404(R) (2007); K. Henderson, C. Ryu, C. MacCormick, and M. G. Boshier, New J. Phys. **11**, 043030 (2009).

[2] C. Ryu, M. F. Andersen, P. Cladé, V. Natarajan, K. Helmerson, and W. D. Phillips, Phys. Rev. Lett. **99**, 260401 (2007).

[3] A. Ramanathan, K. C. Wright, S. R. Muniz, M. Zelan, W. T. Hill, C. J. Lobb, K. Helmerson, W. D. Phillips, and G. K. Campbell, Phys. Rev. Lett. **106**, 130401 (2011).

[4] M. Gildemeister, B. E. Sherlock, and C. J. Foot, Phys. Rev. A **85**, 053401 (2012).

[5] S. Moulder, S. Beattie, R. P. Smith, N. Tammuz, and Z. Hadzibabic, Phys. Rev. A **86**, 013629 (2012).

[6] S. Viefers, P. Koskinen, P. Singha Deo, and M. Manninen, Physica E (Amsterdam, Neth.) **21**, 1 (2004).

[7] M. Manninen, S. Viefers, and S. M. Reimann, Physica E (Amsterdam, Neth.) **46**, 119 (2012).

[8] A. Griesmaier, J. Werner, S. Hensler, J. Stuhler, and T. Pfau, Phys. Rev. Lett. **94**, 160401 (2005); J. Stuhler, A. Griesmaier, T. Koch, M. Fattori, T. Pfau, S. Giovanazzi, P. Pedri, and L. Santos, *ibid.* **95**, 150406 (2005); M. Fattori, T. Koch, S. Goetz, A. Griesmaier, S. Hensler, J. Stuhler, and T. Pfau, Nat. Phys. **2**, 765 (2006); A. Griesmaier, J. Stuhler, T. Koch, M. Fattori, T. Pfau, and S. Giovanazzi, Phys. Rev. Lett. **97**, 250402 (2006).

[9] K.-K. Ni *et al.*, Science **322**, 231 (2008); S. Ospelkaus, K.-K. Ni, G. Quemener, B. Neyenhuis, D. Wang, M. H. G. de Miranda, J. L. Bohn, J. Ye, and D. S. Jin, Phys. Rev. Lett. **104**, 030402 (2010).

[10] T. Lahaye, C. Menotti, L. Santos, M. Lewenstein, and T. Pfau, Rep. Prog. Phys. **72**, 126401 (2009).

[11] G. M. Bruun and E. Taylor, Phys. Rev. Lett. **101**, 245301 (2008).

[12] M. Abad, M. Guilleumas, R. Mayol, M. Pi, and D. M. Jezek, Phys. Rev. A **79**, 063622 (2009).

[13] F. Malet, T. Kristensen, S. M. Reimann, and G. M. Kavoulakis, Phys. Rev. A **83**, 033628 (2011).

[14] M. Abad, M. Guilleumas, R. Mayol, M. Pi, and D. M. Jezek, Phys. Rev. A **81**, 043619 (2010).

[15] F. Malet, G. M. Kavoulakis, and S. M. Reimann, Phys. Rev. A **84**, 043626 (2011).

[16] M. Abad, M. Guilleumas, R. Mayol, M. Pi, and D. M. Jezek, Phys. Rev. A **84**, 035601 (2011).

[17] M. Abad, M. Guilleaumas, R. Mayol, M. Pi, and D. M. Jezek, Europhys. Lett. **94**, 10004 (2011).

[18] M. Abad, M. Guilleaumas, R. Mayol, M. Pi, and D. M. Jezek, Laser Phys. **18**, 648 (2008).

[19] M. Lu, N. Q. Burdick Seo, H. Youn, and B. L. Lev, Phys. Rev. Lett. **107**, 190401 (2011).

[20] S. Zöllner, G. M. Bruun, C. J. Pethick, and S. M. Reimann, Phys. Rev. Lett. **107**, 035301 (2011).

[21] B. Xiong, J. Gong, H. Pu, W. Bao, and B. Li, Phys. Rev. A **79**, 013626 (2009); M. Asad-uz-Zaman and D. Blume, *ibid.* **80**, 053622 (2009).

[22] M. Cozzini, B. Jackson, and S. Stringari, Phys. Rev. A **73**, 013603 (2006).

[23] F. Piazza, L. A. Collins, and A. Smerzi, Phys. Rev. A **80**, 021601 (2009).

[24] R. Dubessy, T. Liennard, P. Pedri, and H. Perrin, Phys. Rev. A **86**, 011602 (2012).

[25] S. J. Woo and Y.-W. Son, Phys. Rev. A **86**, 011604(R) (2012).

[26] R. J. Donnelly and A. L. Fetter, Phys. Rev. Lett. **17**, 747 (1966); A. L. Fetter, Phys. Rev. **153**, 285 (1967).

[27] P. J. Bendt and R. J. Donnelly, Phys. Rev. Lett. **19**, 214 (1967).

[28] J. C. Cremon, G. M. Bruun, and S. M. Reimann, Phys. Rev. Lett. **105**, 255301 (2010).

[29] S. A. Chin and E. Krotscheck, Phys. Rev. E **72**, 036705 (2005).

[30] D. A. Butts and D. S. Rokhsar, Nature (London) **397**, 327 (1999).

[31] F. Bloch, Phys. Rev. A **7**, 2187 (1973).